AIMS Mathematics

http://www.aimspress.com/journal/Math

AIMS Mathematics, 7(7): 12154–12176.
DOI:10.3934/math.2022676
Received: 11 February 2022
Revised: 04 April 2022
Accepted: 13 April 2022
Published: 22 April 2022

Research article

Bifurcation analysis of a food chain chemostat model with Michaelis-Menten functional response and double delays

Xin Xu[1], Yanhong Qiu[1,*], Xingzhi Chen[2], Hailan Zhang[1], Zhiyuan Liang[1] and Baodan Tian[1,*]

[1] College of Mathematics and Physics, Southwest University of Science and Technology, Mianyang, Sichuan 621010, China

[2] College of Mathematics and Statistics, Chongqing University, Chongqing 400000, China

[*] **Correspondence:** Email: yanhongqiu@139.com, tianbaodan@139.com.

Abstract: In this paper, we study a food chain chemostat model with Michaelis-Menten function response and double delays. Applying the stability theory of functional differential equations, we discuss the conditions for the stability of three equilibria, respectively. Furthermore, we analyze the sufficient conditions for the Hopf bifurcation of the system at the positive equilibrium. Finally, we present some numerical examples to verify the correctness of the theoretical analysis and give some valuable conclusions and further discussions at the end of the paper.

Keywords: chemostat model; delay; equilibrium; stability; Hopf bifurcation
Mathematics Subject Classification: 34D05, 37N25, 92B05

1. Introduction

Continuous culture technology is necessary for microbial physiology and biochemistry research, and the chemostat is a continuous culture device that enables microorganisms to grow and reproduce under conditions lower than their maximum growth rate. Typically, it consists of three vessels. The first vessel contains a nutrient substrate that allows the microorganisms to grow sufficiently, and the nutrient substrate is pumped into the second vessel at a constant rate. The second vessel is called the culture vessel, and the mixture of nutrient substrates and microorganisms inside are pumped into the third vessel at the same rate to maintain its capacity.

Since the chemostat model can scientifically describe the continuous culture process of microorganisms, it is widely used to theoretically study the growth of microorganisms in ecological environments, such as rivers and lakes in nature [1–3]. In addition, there is a biological treatment method in waste-water treatment, which usually uses specific microorganisms to decompose harmful substances in waste-water, and the microbe is a bait for another microbe. To this end, some biologists have taken advantage of the chemostat model, which can reasonably describe the complex interactions between biological populations, and have applied it to control the biological waste-water treatment processes, resulting in economic benefits (see [4–6]). Therefore, the study of the chemostat model in waste-water treatment will have crucial academic value and practical significance.

The research on the mathematical model of chemostat can be traced back to the work of Novick and Szilard in reference [7]. Since then, various studies on chemostat models have sprung up (see [8–12]). Generally, a deterministic chemostat model can be expressed by the following differential equations [13],

$$\begin{cases} \frac{ds}{dt} = Q\left(s^0 - s(t)\right) - x(t)p(s(t)), \\ \frac{dx}{dt} = x(t)(p(s(t)) - Q), \end{cases}$$

where $s(t)$ represents the concentration of nutrient substrate; $x(t)$ indicates the density of microorganisms in the chemostat; s^0 stands for the initial concentration of the substrate in the first vessel; Q is the dilution rate; $p(s(t))$ denotes the functional response function of microorganisms from absorbing nutrients to transforming into their own growth rate. One of the most famous functional responses is the Michaelis-Menten functional response [14], which is fully used to describe single-substrate enzymatic reactions. The specific form is as follows,

$$p(s) = \frac{\mu_m s}{K_m + s},$$

where K_m is Michaelis constant, μ_m indicates the reaction speed of the enzyme when the substrate is saturated, and s represents the concentration of substrate.

On the one hand, various organisms in the waste-water treatment ecosystem can generally be divided into three categories: bacteria, algae, and protozoa. Among them, bacteria are the main force of waste-water biological treatment, mainly responsible for the degradation of pollutants; protozoa can prey on free bacteria and reduce the density of bacteria in water [15]. Furthermore, these organisms often have a simple food chain relationship in waste-water treatment systems: organic matter-bacteria-algae-protozoa. Since the waste-water treatment processes mainly rely on such interactions between organisms, it is necessary to consider a chemostat model with a food chain. Recently, a large number of scholars have devoted themselves to studying the chemostat models with a food chain. For example, Li [16] analyzed a predator-prey chemostat model with a general response function under different removal rates and studied the stability and persistence of the population. Wang [17] discussed a stochastic predator-prey chemostat model driven by Markov mechanism conversion and introduced sufficient conditions for the existence of a stable distribution. In particular, Ali [18] made a pretty representative work, which considered a predator-prey food chain chemostat model with Michaelis-Menten functional response. They analyzed the mechanism of chaos in the following model, deduced the mathematical conditions for the existence of periodic orbits, and discussed the microbial dynamics of the system under different conditions. The differential expression is as follows,

$$\begin{cases} \frac{\mathrm{d}x(t)}{\mathrm{d}t} = \frac{m_1 s(t)x(t)}{a_1+s(t)} - Qx(t) - \frac{m_2 x(t)y(t)}{a_2+x(t)}, \\ \frac{\mathrm{d}y(t)}{\mathrm{d}t} = \frac{m_2 x(t)y(t)}{a_2+x(t)} - Qy(t), \\ \frac{\mathrm{d}s(t)}{\mathrm{d}t} = Q\left(s^0 - s(t)\right) - \frac{m_1 s(t)x(t)}{a_1+s(t)}, \end{cases} \tag{1.1}$$

where $s(t)$ indicates the concentration of nutrient substrate; $x(t)$ represents the density of prey-type microorganisms in the chemostat; $y(t)$ stands for the density of predator-type microorganisms in the chemostat; $a_i(i = 1, 2)$ denotes the half-saturation coefficient; m_1 and m_2 show the maximum absorption rate of nutrient $s(t)$ by microorganism $x(t)$ and the maximum growth rate of prey $x(t)$ by predator $y(t)$, respectively.

On the other hand, time delays always exist in the real world. For example, due to the limited switching speed and communication time, there is a time delay in the artificial neural network. Another example is the incubation period between infecting an infectious disease and developing symptoms. Likewise, organisms' uptake and conversion of nutrients are not instantaneous but with a time delay and so on (see [19–23]). Many scholars have studied the effect of these time delays on the dynamic behavior of systems, and the results show that the time delays can lead to stability changes, Hopf bifurcations, and even periodic oscillations, which can help us control and solve practical problems. For example, Zhao [24], Song [25], and Huang [26] established neural network models with time delays and discussed the stability of the system with the time delay as a parameter. Xiao [27], Zhang [28], and Zhu [29] considered time delays in the model with infectious diseases and proved that a more extended time delay would destroy the stability of the system. Song [30], Li [31], and Jiang [32] analyzed the effect of time delays in systems with predator-prey relationships and mainly investigated the stability of periodic solutions for Hopf bifurcations. In particular, Jiang [32] proposed an efficient delayed feedback control scheme for Hopf bifurcation. Similarly, the biological time delay in chemostats has also attracted the attention of biologists and mathematicians. In the ecosystem, there are two types of time delays: One is the time interval between the absorption of nutrients and the consumption of nutrients, which is called discrete delay; the other is that the growth of biological population density is not only related to the density at the current stage, but also related to the population density in the past historical period, which is called the distributed delay. Ruan [33] and Wolkowicz [34] studied a chemostat model with distributed delay and discrete delay, respectively. Tian [35]considered the chemostat model with impulse effects and distributed delays and obtained the conditions for the global asymptotic stability of the system. Sun [36] discussed a chemostat model with a general monotonic response function and two discrete delays. Yu [37] analyzed a stochastic chemostat model with two distributed delays and nonlinear disturbances and obtained the existence, uniqueness, and stability of the positive global solution.

Inspired by the above research background, considering the discrete delay between the absorption and utilization of nutrients by populations with food chain relationships in biological wastewater treatment, based on Ali [18], we further include discrete delays in the modeling. Therefore, compared with other studies with only one delay, we propose a food chain chemostat model with Michaelis-Menten functional response and double delays. Both the delayed effect of prey-type organisms in nutrient decomposition and absorption and the delayed effect of predation are considered, which is novel and valuable. The scheme can be as follows,

$$\begin{cases} \frac{\mathrm{d}x(t)}{\mathrm{d}t} = \frac{m_1 s(t)x(t-\tau_1)}{a_1+s(t)} - Qx(t) - \frac{m_2 x(t-\tau_2)y(t-\tau_2)}{a_2+x(t-\tau_2)}, \\ \frac{\mathrm{d}y(t)}{\mathrm{d}t} = \frac{m_2 x(t-\tau_2)y(t-\tau_2)}{a_2+x(t-\tau_2)} - Qy(t), \\ \frac{\mathrm{d}s(t)}{\mathrm{d}t} = Q\left(s^0 - s(t)\right) - \frac{m_1 s(t)x(t-\tau_1)}{a_1+s(t)}, \end{cases} \tag{1.2}$$

where all parameters are positive constants. Especially, τ_1 indicates the time delay for the conversion of nutrient bases into prey energy, and τ_2 represents the time delay for the conversion of prey into predator energy.

For the convenience of discussion, we make dimensionless processing on some parameters of model (1.2),

$$\bar{x} = \frac{x}{s^0},\ \bar{y} = \frac{y}{s^0},\ \bar{s} = \frac{s}{s^0},\ \bar{t} = Qt,\ \bar{m} = \frac{m}{Q},\ \bar{a} = \frac{a}{s^0}.$$

Let $x(t),\ y(t),\ s(t)$ instead of $\bar{x}(t),\ \bar{y}(t),\ \bar{s}(t)$, and the model we finally studied is as follows,

$$\begin{cases} \frac{dx(t)}{dt} = \frac{m_1 s(t)x(t-\tau_1)}{a_1+s(t)} - x(t) - \frac{m_2 x(t-\tau_2)y(t-\tau_2)}{a_2+x(t-\tau_2)}, \\ \frac{dy(t)}{dt} = \frac{m_2 x(t-\tau_2)y(t-\tau_2)}{a_2+x(t-\tau_2)} - y(t), \\ \frac{ds(t)}{dt} = 1 - s(t) - \frac{m_1 s(t)x(t-\tau_1)}{a_1+s(t)}. \end{cases} \tag{1.3}$$

Next, in Section 2, we will prove the existence of three equilibria in system (1.3). In Section 3, we will discuss the stability of each equilibrium, respectively. In addition, we will analyze the condition for the Hopf bifurcation at the positive equilibrium. In Section 4, we will give some numerical examples to verify the correctness of the theoretical analysis. Finally, combining the results of theoretical analysis and numerical simulation, we will make some conclusions and discussions.

2. Existence of equilibria

Since model (1.3) is a system of delay differential equations, the initial conditions of system (1.3) can be shown as follows.

$$(\psi_1(t), \psi_2(t), \psi_3(t)) \in C_+ = C\left[(-\tau, 0], R^3_+\right), \quad \psi_i(0) > 0, i = 1, 2, 3, \tag{2.1}$$

where $\tau = \max\{\tau_1, \tau_2\}, R^3_+ = \left\{(x(t), y(t), s(t)) \in R^3 \mid x(t) \geqslant 0, y(t) \geqslant 0, s(t) \geqslant 0\right\}$, $\psi_i(t)$ is the initial value function, and C is the Banach space.

Lemma 2.1. For the initial conditions Eq (2.1), there is a unique positive solution $(x(t), y(t), s(t))$ for system (1.3) on $t \geq 0$.

Proof. Since model (1.3) is continuous and the coefficients of system (1.3) satisfy the locally Lipschitz condition, according to Theorem 2.3 in reference [38], we deduce that system (1.3) has a unique solution $(x(t), y(t), s(t))$ for all $t \geq 0$. Moreover, for the initial conditions Eq (2.1), it is easy to obtain that all solutions of system (1.3) are defined on $(0, +\infty)$ and remain positive on $t \geq 0$.

Thus, there is a unique positive solution $(x(t), y(t), s(t))$ for system (1.3) on $t \geq 0$. □

Theorem 2.1. When $m_1 > a_1 + 1$, $m_2 > 1$ and $0 < a_1 < 1$, system (1.3) have three equilibria,

$$E_0(0, 0, 1),\ E_1\left(\frac{a_1}{m_1 - 1}, 0, \frac{m_1 - (a_1 + 1)}{m_1 - 1}\right),\ E_2(x^*, y^*, s^*),$$

where,

$$x^* = \frac{a_2}{m_2 - 1},\ y^* = \frac{(m_2 - 1)(1 + a_1) + a_2(m_1 - 2) - \sqrt{\Delta}}{2(m_2 - 1)},$$

$$s^* = \frac{(1 - a_1)(m_2 - 1) - m_1 a_2 + \sqrt{\Delta}}{2(m_2 - 1)},$$

$$\Delta = (m_2 - a_1 m_2 - a_2 m_1 + a_1 - 1)^2 + 4a_1(1 - m_2)^2 > 0.$$

Proof. For system (1.3), setting the right side equal to 0, we get the corresponding algebraic equations,

$$\begin{cases} x\left(\frac{m_1 s}{a_1+s} - \frac{m_2 y}{a_2+x} - 1\right) = 0, \\ y\left(\frac{m_2 x}{a_2+x} - 1\right) = 0, \\ 1 - s - \frac{m_1 s}{a_1+s}x = 0. \end{cases} \tag{2.2}$$

Obviously, there is a boundary equilibrium $E_0(0,0,1)$ in system (1.3). In addition, when $m_1 > a_1+1$, we easily calculate anothor boundary equilibrium $E_1\left(\frac{m_1-a_1-1}{m_1-1}, 0, \frac{a_1}{m_1-1}\right)$.

Moreover, when $m_1 > a_1 + 1$ and $m_2 > 1$, the predator and prey species will coexist, then we obtain

$$x^* = \frac{a_2}{m_2 - 1}. \tag{2.3}$$

Substituting Eq (2.3) into Eq (2.2), we have

$$(1 - m_2)s^{*2} + (m_2 - a_1 m_2 - a_2 m_1 + a_1 - 1)s^* - a_1(1 - m_2) = 0. \tag{2.4}$$

Since $0 < a_1 < 1$, according to the relationship between the roots and coefficients of quadratic equations in one variable, we have $s_1^* s_2^* = -a_1 < 0$, then we get the unique positive root of Eq (2.4),

$$s^* = \frac{(1 - a_1)(m_2 - 1) - m_1 a_2 + \sqrt{\Delta}}{2(m_2 - 1)}.$$

Owing to $x^* + y^* + s^* = 1$, we get

$$y^* = 1 - s^* - x^* = \frac{(m_2 - 1)(1 + a_1) + a_2(m_1 - 2) - \sqrt{\Delta}}{2(m_2 - 1)} > 0.$$

Therefore, when $m_1 > a_1 + 1$, $m_2 > 1$ and $0 < a_1 < 1$, system (1.3) always has three equilibria,

$$E_0(0,0,1),\ E_1\left(\frac{a_1}{m_1 - 1}, 0, \frac{m_1 - (a_1 + 1)}{m_1 - 1}\right),\ E_2(x^*, y^*, s^*),$$

where,

$$x^* = \frac{a_2}{m_2 - 1},\ y^* = \frac{(m_2 - 1)(1 + a_1) + a_2(m_1 - 2) - \sqrt{\Delta}}{2(m_2 - 1)},$$

$$s^* = \frac{(1 - a_1)(m_2 - 1) - m_1 a_2 + \sqrt{\Delta}}{2(m_2 - 1)}.$$

□

3. Stability and Hopf bifurcation

3.1. The equilibrium $E_0(0,0,1)$

Firstly, we will focus on the stability of equilibrium $E_0(0,0,1)$.

Theorem 3.1.

1) When $m_1 < a_1 + 1$, the equilibrium $E_0(0,0,1)$ is locally asymptotically stable.

2) When $m_1 > a_1 + 1$, the equilibrium $E_0(0,0,1)$ is unstable.

Proof. Let $x_1 = x$, $y_1 = y$ and $s_1 = s - 1$, and we can get the linearized system of system (1.3) at the equilibrium $E_0(0,0,1)$,

$$\begin{cases} \frac{dx_1(t)}{dt} = \frac{m_1 x_1(t-\tau_1)}{a_1+1} - x_1(t), \\ \frac{dy_1(t)}{dt} = -y_1(t), \\ \frac{ds_1(t)}{dt} = -s_1(t) - \frac{m_1 x_1(t-\tau_1)}{a_1+1}. \end{cases} \tag{3.1}$$

Then, we obtain the characteristic equation of system (3.1) at the equilibrium $E_0(0,0,1)$,

$$J(E_0) = \begin{vmatrix} \lambda + 1 - \frac{m_1}{a_1+1}e^{-\lambda\tau_1} & 0 & 0 \\ 0 & \lambda + 1 & 0 \\ \frac{m_1}{a_1+1}e^{-\lambda\tau_1} & 0 & \lambda + 1 \end{vmatrix} = (\lambda+1)^2[\lambda + 1 - \frac{m_1}{a_1+1}e^{-\lambda\tau_1}]. \tag{3.2}$$

Obviously, $\lambda_{1,\,2} = -1$ and λ_3 satisfies the following equation,

$$f(\lambda_3) = \lambda_3 + 1 - \frac{m_1}{a_1+1}e^{-\lambda_3\tau_1} = 0. \tag{3.3}$$

On the one hand, when $m_1 < a_1 + 1$, we claim that $Re(\lambda_3) < 0$. Otherwise, if $Re(\lambda_3) \geq 0$, we obtain

$$Re(\lambda_3) = -1 + \frac{m_1}{a_1+1}e^{-Re(\lambda_3)\tau_1}\cos(Im(\lambda_3)\tau_1) \leq \frac{m_1}{a_1+1} - 1 < 0,$$

which leads to a contradiction. Thus, all solutions of Eq (3.3) have negative real parts.

On the other hand, when $m_1 > a_1 + 1$, we have

$$f(0) = 1 - \frac{m_1}{a_1+1} < 0, \quad \lim_{\lambda_3 \to +\infty} f(\lambda_3) = +\infty > 0.$$

Hence, there is a $\lambda_3^* > 0$ such that $f(\lambda_3^*) = 0$, then Eq (3.3) must have a positive root.

Therefore, we conclude that when $m_1 < a_1 + 1$, all solutions of Eq.(3.2) have negative real parts, then the equilibrium $E_0(0,0,1)$ is locally asymptotically stable; when $m_1 > a_1 + 1$, the solutions of Eq (3.2) will have a positive root, then the equilibrium $E_0(0,0,1)$ is unstable. □

3.2. *The equilibrium* $E_1\left(\frac{a_1}{m_1-1}, 0, \frac{m_1-(a_1+1)}{m_1-1}\right)$

Secondly, we will discuss the stability of equilibrium $E_1\left(\frac{a_1}{m_1-1}, 0, \frac{m_1-(a_1+1)}{m_1-1}\right)$.

Define,

$$x_1^* = \frac{a_1}{m_1-1}, \; s_1^* = \frac{m_1-(a_1+1)}{m_1-1}, \; \theta_1 = \frac{m_1 a_1 x_1^*}{(a_1+s_1^*)^2},$$

$$\theta_2 = \frac{m_2 x_1^*}{a_2 + x_1^*} = \frac{m_2(m_1 - a_1 - 1)}{a_2(m_1-1) + m_2(m_1 - a_1 - 1)}.$$

Theorem 3.2. When $m_1 > a_1 + 1$, the equilibrium $E_1(x_1^*, 0, s_1^*)$ is locally asymptotically stable.

Proof. Let $x_1 = x - x_1^*$, $y_1 = y - 0$ and $s_1 = s - s_1^*$, by variable substitution and $\frac{m_1 s_1^*}{a_1+s_1^*} = 1$, and we obtain

$$\begin{cases} \frac{dx_1(t)}{dt} = -x_1(t) + x_1(t-\tau_1) + \frac{a_1 x_1^*}{m_1(s_1^*)^2}s_1(t) - \frac{m_2 x_1^*}{a_2+x_1^*}y_1(t-\tau_2), \\ \frac{dy_1(t)}{dt} = \frac{m_2 x_1^*}{a_2+x_1^*}y_1(t-\tau_2) - y_1(t), \\ \frac{ds_1(t)}{dt} = -\left(1 + \frac{a_1 x_1^*}{m_1(s_1^*)^2}\right)s_1(t) - x_1(t-\tau_1). \end{cases} \tag{3.4}$$

Then, we get the characteristic equation of system (3.4) at the equilibrium $E_1\left(x_1^*, 0, s_1^*\right)$,

$$\begin{aligned} J(E_1) &= \begin{vmatrix} \lambda + 1 - e^{-\lambda\tau_1} & \theta_2 e^{-\lambda\tau_2} & -\theta_1 \\ 0 & \lambda + 1 - \theta_2 e^{-\lambda\tau_2} & 0 \\ e^{-\lambda\tau_1} & 0 & \lambda + 1 + \theta_1 \end{vmatrix} \\ &= (\lambda + 1)(\lambda + 1 - \theta_2 e^{-\lambda\tau_2})(\lambda + 1 + \theta_1 - e^{-\lambda\tau_1}). \end{aligned} \tag{3.5}$$

Obviously, $\lambda_a = -1$ is a negative eigenvalue.

On the one hand, the second eigenvalue satisfies the following equation,

$$\lambda_b = \theta_2 e^{-\lambda_b\tau_2} - 1. \tag{3.6}$$

When $m_1 > a_1 + 1$, we obtain $Re(\lambda_b) < 0$. On the contrary, if $Re(\lambda_b) \geq 0$, we get

$$Re(\lambda_b) = -1 + \theta_2 e^{-Re(\lambda_b)\tau_2} \cos(Im(\lambda_b)\tau_2) \leq \theta_2 - 1 < 0,$$

which leads to a contradiction. Thus, all eigenvalues of Eq (3.6) have negative real parts.

On the other hand, the third eigenvalue satisfies the following equation,

$$\lambda_c = e^{-\lambda_c\tau_1} - \theta_1 - 1. \tag{3.7}$$

When $m_1 > a_1 + 1$, we claim that $Re(\lambda_c) < 0$. Otherwise, if $Re(\lambda_c) \geq 0$, we have

$$Re(\lambda_c) = -1 - \theta_1 + e^{-Re(\lambda_c)\tau_1} \cos(Im(\lambda_c)\tau_1) \leq -\theta_1 = -\frac{m_1(a_1)^2}{(m_1 - 1)(a_1 + s_1^*)^2} < 0,$$

which leads to a contradiction. Thus, all eigenvalues of Eq (3.7) have negative real parts.

Therefore, we conclude that when $m_1 > a_1 + 1$, all solutions of Eq (3.5) have negative real parts, then the equilibrium $E_1\left(x_1^*, 0, s_1^*\right)$ is locally asymptotically stable. □

3.3. *The positive equilibrium $E_2(x^*, y^*, s^*)$*

Next, we will analyze the stability of the positive equilibrium $E_2(x^*, y^*, s^*)$.

Define,

$$\theta_3 = \frac{m_1 s^*}{a_1 + s^*},\ \theta_4 = \frac{m_1 a_1 x^*}{(a_1 + s^*)^2},\ \theta_5 = \frac{-a_2 y^*}{m_2(x^*)^2} = \frac{-(m_1 - 1)(m_2 - 1)}{m_2} + \frac{a_1 m_1(m_2 - 1)}{m_2(a_1 + s)},$$

$$\beta_1 = \theta_4 + 3,\ \beta_2 = 2\theta_4 + 3,\ \beta_3 = \theta_4 + 1,\ \beta_4 = -\theta_3, \beta_5 = -2\theta_3,\ \beta_6 = -\theta_3,$$

$$\beta_7 = -\theta_5 - 1,\ \beta_8 = -\theta_4\theta_5 - 2\theta_5 - \theta_4 - 2,\ \beta_9 = -\theta_4\theta_5 - \theta_4 - \theta_5 - 1,\ \beta_{10} = \beta_{11} = \theta_3.$$

Let $x_1 = x - x^*$, $y_1 = y - y^*$ and $s_1 = s - s^*$, by variable substitution and $\frac{m_2 x^*}{a_2 + x^*} = 1$, and we obtain the following system,

$$\begin{cases} \frac{\mathrm{d}x_1(t)}{\mathrm{d}t} = -x_1(t) + \frac{m_1 s^*}{a_1 + s^*} x_1(\tau - \tau_1) - \frac{y^* a_2}{m_2(x^*)^2} x_1(\tau - \tau_2) - y_1(\tau - \tau_2) + \frac{m_1 a_1 x^*}{(a_1 + s^*)^2} s_1(t), \\ \frac{\mathrm{d}y_1(t)}{\mathrm{d}t} = \frac{y^* a_2}{m_2(x^*)^2} x_1(\tau - \tau_2) - y_1(t) + y_1(\tau - \tau_2), \\ \frac{\mathrm{d}s_1(t)}{\mathrm{d}t} = -\frac{m_1 s^*}{a_1 + s^*} x_1(\tau - \tau_1) - s_1(t) - \frac{m_1 a_1 x^*}{(a_1 + s^*)^2} s_1(t). \end{cases} \tag{3.8}$$

Then, we get the characteristic equation of system (3.8) at the positive equilibrium $E_2(x^*, y^*, s^*)$,

$$J(E_2) = \begin{vmatrix} \lambda + 1 - \theta_3 e^{-\lambda\tau_1} - \theta_5 e^{-\lambda\tau_2} & e^{-\lambda\tau_2} & -\theta_4 \\ \theta_5 e^{-\lambda\tau_2} & \lambda + 1 - e^{-\lambda\tau_2} & 0 \\ \theta_3 e^{-\lambda\tau_1} & 0 & \lambda + 1 + \theta_4 \end{vmatrix}$$
$$= H_0(\lambda) + H_1(\lambda)e^{-\lambda\tau_1} + H_2(\lambda)e^{-\lambda\tau_2} + H_3(\lambda)e^{-\lambda\tau_1}e^{-\lambda\tau_2}, \tag{3.9}$$

where,

$$H_0(\lambda) = \lambda^3 + \beta_1\lambda^2 + \beta_2\lambda + \beta_3,\ H_1(\lambda) = \beta_4\lambda^2 + \beta_5\lambda + \beta_6,$$
$$H_2(\lambda) = \beta_7\lambda^2 + \beta_8\lambda + \beta_9,\ H_3(\lambda) = \beta_{10}\lambda + \beta_{11}.$$

3.3.1. The case $\tau_1 = \tau_2 = 0$

Theorem 3.3. When $\tau_1 = \tau_2 = 0$, $m_1 > a_1 + 1$, $m_2 > 1$, $0 < a_1 < 1$, $\beta_1 + \beta_4 + \beta_7 > 0$, $\beta_3 + \beta_9 > 0$ and $(\beta_1 + \beta_4 + \beta_7)(\beta_2 + \beta_5 + \beta_8 + \beta_{10}) > (\beta_3 + \beta_9)$, the positive equilibrium $E_2(x^*, y^*, s^*)$ is locally asymptotically stable.

Proof. Let $\tau_1 = \tau_2 = 0$, based on Eq (3.9), and we obtain

$$f(\lambda) = \lambda^3 + (\beta_1 + \beta_4 + \beta_7)\lambda^2 + (\beta_2 + \beta_5 + \beta_8 + \beta_{10})\lambda + (\beta_3 + \beta_9) = 0. \tag{3.10}$$

Since $\beta_1 + \beta_4 + \beta_7 > 0, \beta_3 + \beta_9 > 0$ and $(\beta_1 + \beta_4 + \beta_7)(\beta_2 + \beta_5 + \beta_8 + \beta_{10}) > (\beta_3 + \beta_9)$, we get

$$\begin{aligned} \mathcal{A}_1 &= (\beta_1 + \beta_4 + \beta_7) > 0, \\ \mathcal{A}_2 &= \begin{vmatrix} (\beta_1 + \beta_4 + \beta_7) & 1 \\ (\beta_3 + \beta_9) & (\beta_2 + \beta_5 + \beta_8 + \beta_{10}) \end{vmatrix} \\ &= (\beta_1 + \beta_4 + \beta_7)(\beta_2 + \beta_5 + \beta_8 + \beta_{10}) - (\beta_3 + \beta_9) > 0, \\ \mathcal{A}_3 &= \begin{vmatrix} (\beta_1 + \beta_4 + \beta_7) & 1 & 0 \\ (\beta_3 + \beta_9) & (\beta_2 + \beta_5 + \beta_8 + \beta_{10}) & (\beta_1 + \beta_4 + \beta_7) \\ 0 & 0 & (\beta_3 + \beta_9) \end{vmatrix} \\ &= (\beta_3 + \beta_9)((\beta_1 + \beta_4 + \beta_7)(\beta_2 + \beta_5 + \beta_8 + \beta_{10}) - (\beta_3 + \beta_9)) \\ &= (\beta_3 + \beta_9)\mathcal{A}_2 > 0. \end{aligned} \tag{3.11}$$

Utilizing Routh-Hurwitz criterion [39], we conclude that when $\tau_1 = \tau_2 = 0$, all roots of Eq (3.10) have negative real parts. Therefore, when $\tau_1 = \tau_2 = 0$ and the parameters satisfy the conditions of Theorem 3.3, the positive equilibrium $E_2(x^*, y^*, s^*)$ is locally asymptotically stable. □

3.3.2. The case $\tau_1 > 0$ and $\tau_2 = 0$

When $\tau_1 > 0, \tau_2 = 0$, based on Eq (3.9), we obtain

$$f(\lambda) = H_4(\lambda) + H_5(\lambda)e^{-\lambda\tau_1} = 0, \tag{3.12}$$

where,

$$H_4(\lambda) = \lambda^3 + (\beta_1 + \beta_7)\lambda^2 + (\beta_2 + \beta_8)\lambda + \beta_3 + \beta_9,\ H_5(\lambda) = \beta_4\lambda^2 + (\beta_5 + \beta_{10})\lambda.$$

Let $\lambda = i\omega$, and we get

$$E_1 + iF_1 + (E_2 + iF_2)(\cos\omega\tau_1 - isin\omega\tau_1) = 0,$$

where,

$$E_1 = -(\beta_1 + \beta_7)\omega^2 + \beta_3 + \beta_9, \quad F_1 = -\omega^3 + (\beta_2 + \beta_8)\,\omega,$$

$$E_2 = -\beta_4\omega^2, \quad F_2 = (\beta_5 + \beta_{10})\,\omega.$$

Separating the real and imaginary parts, we have

$$\begin{cases} E_2\cos\omega\tau_1 + F_2\sin\omega\tau_1 = -E_1, \\ F_2\cos\omega\tau_1 - E_2\sin\omega\tau_1 = -F_1. \end{cases} \tag{3.13}$$

Adding the squares of two equations, we obtain

$$(-\beta_4\omega^2)^2 + ((\beta_5 + \beta_{10})\omega)^2 = (-(\beta_1 + \beta_7)\omega^2 + \beta_3 + \beta_9)^2 + (-\omega^3 + (\beta_2 + \beta_8)\omega)^2. \tag{3.14}$$

Let $z = \omega^2$, and we get

$$h(z) = z^3 + pz^2 + qz + r = 0, \tag{3.15}$$

and $h'(z) = 3z^2 + 2pz + q,\ h''(z) = 6z + 2p$,
where,

$$p = (\beta_1 + \beta_7)^2 - \beta_4{}^2 - 2\beta_2 - 2\beta_8,\ q = (\beta_2 + \beta_8)^2 - (\beta_5 + \beta_{10})^2 - 2(\beta_1 + \beta_7)(\beta_3 + \beta_9),$$

$$r = (\beta_3 + \beta_9)^2 > 0.$$

For convenience, we let $\Delta_1 = p^2 - 3q$, then two roots of the equation $h'(z) = 0$ can be expressed as $z_1^* = \frac{-p-\sqrt{\Delta_1}}{3}, z_2^* = \frac{-p+\sqrt{\Delta_1}}{3}$.

Theorem 3.4. When $\tau_1 > 0, \tau_2 = 0$, $m_1 > a_1 + 1$, $m_2 > 1$ and $0 < a_1 < 1$, we can get the following conclusions.

1) If $\beta_1 + \beta_4 + \beta_7 > 0$, $\beta_3 + \beta_9 > 0$, $(\beta_1 + \beta_4 + \beta_7)(\beta_2 + \beta_5 + \beta_8 + \beta_{10}) > (\beta_3 + \beta_9)$ and $p^2 - 3q \le 0$, for any $\tau_1 > 0, \tau_2 = 0$, the positive equilibrium $E_2(x^*, y^*, s^*)$ is locally asymptotically stable.
2) If the system parameters do not satisfy the conditions of Theorem 3.3, $q < 0$ and $h(z_2^*) \le 0$, as τ_1 increases, the stability of the positive equilibrium $E_2(x^*, y^*, s^*)$ will change a finite number of times and eventually become unstable. Especially, there is a $\tau_1^* > 0$.
   - When $0 \le \tau_1 < \tau_1^*$ and $\tau_2 = 0$, the positive equilibrium $E_2(x^*, y^*, s^*)$ is unstable.
   - When $\tau_1 = \tau_1^*$ and $\tau_2 = 0$, system (1.3) will undergo a Hopf bifurcation for the first time.
   - When $\tau_1 > \tau_1^*$ and $\tau_2 = 0$, the positive equilibrium $E_2(x^*, y^*, s^*)$ is stable.

Proof. (1) Since $\Delta_1 = p^2 - 3q \le 0$, we obtain $h'(\frac{z_1^*+z_2^*}{2}) \ge 0$ and $h'(z) > 0 (z \ne \frac{z_1^*+z_2^*}{2})$, which indicates that $h(z)$ is monotone increasing. In addition, combining with $h(0) = r > 0$, we obtain Eq (3.15) does not have real roots. Then Eq (3.14) does not have real roots, and Eq (3.12) does not have a root that can cross the imaginary axis.

Moreover, as a result of Corollary 2.4 from reference [40], we know that when $\tau_1 > 0$, the sum of the positive real parts of the roots of Eq (3.10) and Eq (3.12) is equal. Since $\beta_1 + \beta_4 + \beta_7 > 0, \beta_3 + \beta_9 > 0$ and $(\beta_1 + \beta_4 + \beta_7)(\beta_2 + \beta_5 + \beta_8 + \beta_{10}) > (\beta_3 + \beta_9)$, based on the analysis of Theorem 3.3, we can obtain that the sum of positive real parts of the roots of Eq (3.10) is equal to 0, then all the roots of Eq (3.12) only have negative real parts.

Therefore, we can conclude that when $m_1 > a_1 + 1, m_2 > 1, 0 < a_1 < 1, \beta_1 + \beta_4 + \beta_7 > 0$, $\beta_3 + \beta_9 > 0$, $(\beta_1 + \beta_4 + \beta_7)(\beta_2 + \beta_5 + \beta_8 + \beta_{10}) > (\beta_3 + \beta_9)$ and $p^2 - 3q \leq 0$, for any $\tau_1 > 0$ and $\tau_2 = 0$, the positive equilibrium $E_2(x^*, y^*, s^*)$ is locally asymptotically stable.

(2) Since the parameters of system (1.3) do not satisfy the conditions of Theorem 3.3, by the first case of Theorem 3.4, we get $E_2(x^*, y^*, s^*)$ is unstable. In addition, when $q < 0$, we obtain $\Delta_1 = p^2 - 3q > 0$, then the equation $h^{'}(z) = 0$ has two real roots and $z_2^* > 0$. Moreover, we can easily get $h^{''}(z_1^*) = -2\sqrt{\Delta_1} < 0, h^{''}(z_2^*) = 2\sqrt{\Delta_1} > 0$. Thus, z_1^* and z_2^* are the maximum and minimum points of the equation $h^{'}(z) = 0$, respectively.

If $h(z_2^*) = 0$, $z_2^* > 0$ is the positive real root of Eq (3.15); if $h(z_2^*) < 0$, there must exist $z^* > 0$ such that $h(z^*) = 0$. Thus, when $q < 0$ and $h(z_2^*) \leq 0$, Eq (3.15) always has positive real roots. Then, Eq (3.14) has at least a pair of real roots that are opposite to each other, and Eq (3.12) has at least a pair of conjugate imaginary roots $\pm i\omega_0$ ($\omega_0 = \sqrt{z^*}$).

Furthermore, based on Eq (3.13), we obtain

$$\cos\omega\tau_1 = \frac{-E_1E_2 - F_1F_2}{E_2^2 + F_2^2}, \ \sin\omega\tau_1 = \frac{F_1E_2 - E_1F_2}{E_2^2 + F_2^2}.$$

Hence,

$$\tau_1^j = \frac{1}{\omega_0}\left[\arccos\left(\frac{-E_1E_2 - F_1F_2}{E_2^2 + F_2^2}\right) + 2j\pi\right], j = 0, 1, 2...$$

According to Hopf bifurcation theory [41], we can describe the bifurcation point as $\tau_1^* = \min\left(\tau_1^j\right), j = 0, 1, 2...$

When $\tau_1 = \tau_1^*$, we get

$$\frac{d\lambda}{d\tau_1} = \frac{\lambda H_5(\lambda)e^{-\lambda\tau_1}}{H_4'(\lambda) + H_5'(\lambda)e^{-\lambda\tau_1} - \tau_1 H_5(\lambda)e^{-\lambda\tau_1}} = \frac{\Phi}{\Psi}.$$

Let $\lambda = i\omega$, and we obtain

$$\mathrm{Re}\left[\frac{d\lambda}{d\tau}\right]_{\omega=\omega_0}^{\tau_1=\tau_1^*} = \frac{\Phi_1\Psi_1 + \Phi_1\Psi_2}{\Psi_1^2 + \Psi_2^2} \neq 0,$$

where,

$$\Phi_1 = \omega_0 E_2 \sin\omega_0\tau_1^* - \omega_0 F_2 \cos\omega_0\tau_1^*, \ \Phi_2 = \omega_0 F_2 \sin\omega_0\tau_1^* + \omega_0 E_2 \cos\omega_0\tau_1^*,$$

$$\Psi_1 = E_1' - (E_2' + \tau_1^* F_2)\sin\omega_0\tau_1^* + (F_2' - \tau_1^* E_2)\cos\omega_0\tau_1^*,$$

$$\Psi_2 = F_1' - (F_2' - \tau_1^* E_2)\sin\omega_0\tau_1^* - (E_2' - \tau_1^* F_2)\cos\omega_0\tau_1^*,$$

$$E_1' = -2\omega_0(\beta_1 + \beta_7), \ \ F_1' = -3{\omega_0}^2 + \beta_2 + \beta_8,, \ E_2' = -2\beta_4, \ \ F_2' = \beta_5 + \beta_{10}.$$

Therefore, making use of Hopf bifurcation theory [41], we obtain when $q < 0$, $h(z_2^*) \leq 0$ and the system parameters do not satisfy the conditions of Theorem 3.3, as τ_1 increases, the stability of the positive equilibrium $E_2(x^*, y^*, s^*)$ will change at most a limited number of times and eventually become unstable [42]. Especially, there is a ${\tau_1}^*$ such that when $0 \leq \tau_1 < \tau_1^*$ and $\tau_2 = 0$, the positive equilibrium $E_2(x^*, y^*, s^*)$ is unstable; when $\tau_1 = \tau_1^*$ and $\tau_2 = 0$, system (1.3) will undergo a Hopf bifurcation for the first time; when $\tau_1 > \tau_1^*$ and $\tau_2 = 0$, the positive equilibrium $E_2(x^*, y^*, s^*)$ is stable. □

3.3.3. The case $\tau_1 = 0$ and $\tau_2 > 0$

When $\tau_1 = 0, \tau_2 > 0$, based on Eq (3.9), we have

$$f(\lambda) = H_6(\lambda) + H_7(\lambda)e^{-\lambda\tau_2} = 0, \tag{3.16}$$

where,

$$H_6(\lambda) = \lambda^3 + (\beta_1 + \beta_4)\lambda^2 + (\beta_2 + \beta_5)\lambda + \beta_3 + \beta_6,\ H_7(\lambda) = \beta_7\lambda^2 + (\beta_8 + \beta_{10})\lambda + \beta_9 + \beta_{11}.$$

Let $\lambda = i\omega$, and we get

$$E_3 + iF_3 + (E_4 + iF_4)(\cos\omega\tau_2 - i\sin\omega\tau_2) = 0,$$

where,

$$E_3 = -(\beta_1 + \beta_4)\omega^2 + \beta_3 + \beta_6,\quad F_3 = -\omega^3 + (\beta_2 + \beta_5)\,\omega,$$
$$E_4 = -\beta_7\omega^2 + \beta_9 + \beta_{11},\quad F_4 = (\beta_8 + \beta_{10})\,\omega.$$

Separating the real and imaginary parts, we obtain

$$\begin{cases} E_4\cos\omega\tau_2 + F_4\sin\omega\tau_2 = -E_3, \\ F_4\cos\omega\tau_2 - E_4\sin\omega\tau_2 = -F_3. \end{cases} \tag{3.17}$$

Adding the squares of two equations, we have

$$(-\beta_7\omega^2 + \beta_9 + \beta_{11})^2 + ((\beta_8 + \beta_{10})\omega)^2 = (-(\beta_1 + \beta_4)\omega^2 + \beta_3 + \beta_6)^2 + (-\omega^3 + (\beta_2 + \beta_5)\omega)^2. \tag{3.18}$$

Let $n = \omega^2$, and we obtain

$$h(n) = n^3 + un^2 + vn + m, \tag{3.19}$$

and $h'(n) = 3n^2 + 2un + v,\ h''(n) = 6n + 2u$,
where,

$$u = (\beta_1 + \beta_4)^2 - {\beta_7}^2 - 2\beta_2 - 2\beta_5,$$
$$v = (\beta_2 + \beta_5)^2 - (\beta_8 + \beta_{10})^2 + 2\beta_7(\beta_9 + \beta_{11}) - 2(\beta_1 + \beta_4)(\beta_3 + \beta_6),$$
$$m = (\beta_3 + \beta_6)^2 - (\beta_9 + \beta_{11})^2 = -\theta_5(\theta_4 + 1)(-2\theta_3 + (1 + \theta_4)(\theta_5 + 2)).$$

For convenience, we let $\Delta_2 = u^2 - 3v$, then two roots of the equation $h'(n) = 0$ can be expressed as $n_1^* = \frac{-u-\sqrt{\Delta_2}}{3}, n_2^* = \frac{-u+\sqrt{\Delta_2}}{3}$.

Theorem 3.5. When $\tau_1 = 0$, $\tau_2 > 0$, $m_1 > a_1 + 1$, $m_2 > 1$ and $0 < a_1 < 1$, we have the following conclusions.

1) If $v < 0$, $h(n_2^*) \le 0$ and the parameters of system (1.3) do not satisfy the conditions of Theorem 3.3, for any $\tau_1 = 0,\ \tau_2 > 0$, the positive equilibrium $E_2(x^*, y^*, s^*)$ is unstable.
2) If $\beta_1 + \beta_4 + \beta_7 > 0$, $\beta_3 + \beta_9 > 0$, $(\beta_1 + \beta_4 + \beta_7)(\beta_2 + \beta_5 + \beta_8 + \beta_{10}) > (\beta_3 + \beta_9)$, $v < 0$ and $h(n_2^*) \le 0$, there is a $\tau_2^* > 0$.
   - When $\tau_1 = 0$ and $0 \le \tau_2 < \tau_2^*$, the positive equilibrium $E_2(x^*, y^*, s^*)$ is locally asymptotically stable.

- When $\tau_1 = 0$ and $\tau_2 = \tau_2^*$, system (1.3) will undergo a Hopf bifurcation.
- When $\tau_1 = 0$ and $\tau_2 > \tau_2^*$, the positive equilibrium $E_2(x^*, y^*, s^*)$ is unstable.

Proof. (1) Since $v < 0$ and $h(n_2^*) \leq 0$, similar to Theorem 3.4.(2), we obtain that Eq (3.19) always has positive real roots. Then, Eq (3.18) has at least a pair of real roots which are opposite to each other, and Eq (3.16) has at least a pair of conjugate imaginary roots. In addition, since the parameters of system (1.3) do not satisfy the conditions of Theorem 3.3, by the Corollary 2.4 from reference [40], we obtain when $\tau_1 = 0$ and $\tau_2 > 0$, the sum of the positive real parts of the roots of Eq (3.16) and Eq (3.10) is equal. Moreover, by the analysis of Theorem 3.3, we know that when the parameters of system (1.3) do not satisfy the conditions of Theorem 3.3, all roots of Eq (3.10) must have positive real parts, then all roots of Eq (3.16) have positive real part.

Therefore, we conclude that when $v < 0$, $h(n_2^*) \leq 0$ and the parameters of system (1.3) do not satisfy the conditions of Theorem 3.3, for any $\tau_1 = 0,\ \tau_2 > 0$, the positive equilibrium $E_2(x^*, y^*, s^*)$ is unstable.

Furthermore, based on Eq (3.17), we obtain

$$\cos\omega\tau_2 = \frac{-E_3E_4 - F_3F_4}{E_4^2 + F_4^2},\ \ \sin\omega\tau_2 = \frac{F_3E_4 - E_3F_4}{E_4^2 + F_4^2}.$$

Hence,

$$\tau_2^j = \frac{1}{\omega_0}\left[\arccos\left(\frac{-E_3E_4 - F_3F_4}{E_4^2 + F_4^2}\right) + 2j\pi\right], j = 0, 1, 2... \tag{3.20}$$

Similarly, according to Hopf bifurcation theory [41], we can describe the bifurcation point as $\tau_2^* = \min(\tau_2^j)$, $j = 0, 1, 2...$

When $\tau_2 = \tau_2^* > 0$, we obtain

$$\frac{d\lambda}{d\tau_2} = \frac{\lambda H_7(\lambda)e^{-\lambda\tau_2}}{H_6'(\lambda) + H_7'(\lambda)e^{-\lambda\tau_2} - \tau_2 H_7(\lambda)e^{-\lambda\tau_2}} = \frac{\Lambda}{\Theta}.$$

Let $\lambda = i\omega$, and we obtain

$$\mathrm{Re}\left[\frac{d\lambda}{d\tau_2}\right]_{\omega=\omega_0}^{\tau_2={\tau_2}^*} = \frac{\Lambda_1\Theta_1 + \Lambda_2\Theta_2}{\Lambda_1^2 + \Lambda_2^2} \neq 0,$$

where,

$$\Lambda_1 = \omega_0 E_4 \sin\omega_0\tau_2^* - \omega_0 F_4 \cos\omega_0\tau_2^*,\ \Lambda_2 = \omega_0 F_4 \sin\omega_0\tau_2^* + \omega_0 E_4 \cos\omega_0\tau_2^*,$$

$$\Theta_1 = E_3' - (E_4' + \tau_2^* F_4)\sin\omega_0\tau_2^* + (F_4' - \tau_2^* E_4)\cos\omega_0\tau_2^*,$$

$$\Theta_2 = F_3' - (F_4' - \tau_2^* E_4)\sin\omega_0\tau_2^* - (E_4' + \tau_2^* F_4)\cos\omega_0\tau_2^*,$$

$$E_3' = -2\omega_0(\beta_1 + \beta_4),\ \ F_3' = -3{\omega_0}^2 + \beta_2 + \beta_5,\ E_4' = -2\omega_0\beta_7,\ \ F_4' = \beta_8 + \beta_{10}.$$

(2) When $\tau_1 = 0$ and $0 \leq \tau_2 < \tau_2^*$, based on the above analysis, we know that when $v < 0$ and $h(n_2^*) \leq 0$, Eq (3.19) has at least a pair of conjugate imaginary roots. In addition, since $\beta_1 + \beta_4 + \beta_7 > 0$, $\beta_3 + \beta_9 > 0$ and $(\beta_1 + \beta_4 + \beta_7)(\beta_2 + \beta_5 + \beta_8 + \beta_{10}) > (\beta_3 + \beta_9)$, by Theorem 3.3 and the Corollary 2.4 from reference [40], we obtain when $\tau_1 = 0$ and $0 \leq \tau_2 < \tau_2^*$, the sum of the positive real parts of the roots of Eq (3.16) and Eq (3.10) is equal to 0, then all the roots of Eq (3.16) only have negative real parts. Thus, when $\tau_1 = 0,\ 0 \leq \tau_2 < \tau_2^*,\ v < 0,\ h(n_2^*) \leq 0, \beta_1 + \beta_4 + \beta_7 > 0,\ \beta_3 + \beta_9 > 0$ and

$(\beta_1+\beta_4+\beta_7)(\beta_2+\beta_5+\beta_8+\beta_{10}) > (\beta_3+\beta_9)$, the positive equilibrium $E_2(x^*, y^*, s^*)$ is locally asymptotically stable.

When $\tau_1 = 0$ and $\tau_2 = \tau_2^*$, utilizing the conclusion of reference [43], we obtain $signRe(\frac{d\lambda}{d\tau_2})\Big|_{\lambda=\pm i\omega_0} = sign(h'(z)) = sign(h'(\omega^2))$. Since $v < 0$ and $h(n_2^*) \leq 0$, there must exist $n^* > 0$ such that $h'(n_2^*) = 0$. Thus, when $0 < n_2^* < n$, we get $h'(n) > 0$, then $signRe(\frac{d\lambda}{d\tau_2})\Big|_{\lambda=\pm i\omega_0} = 1 > 0$. Thus, when $\tau_1 = 0, \tau_2 = \tau_2^*$, $v < 0$, $h(n_2^*) \leq 0$, $\beta_1+\beta_4+\beta_7 > 0$, $\beta_3+\beta_9 > 0$ and $(\beta_1+\beta_4+\beta_7)(\beta_2+\beta_5+\beta_8+\beta_{10}) > (\beta_3+\beta_9)$, system (1.3) will undergo a Hopf bifurcation.

In addition, when delay parameter τ_2 increases from τ_2^*, the characteristic root of characteristic Eq (3.16) will cross the imaginary axis [44]. It means system (1.3) eventually become unstable. Thus, when $\tau_1 = 0, \tau_2 > \tau_2^*, v < 0, h(n_2^*) \leq 0, \beta_1+\beta_4+\beta_7 > 0$, $\beta_3+\beta_9 > 0$ and $(\beta_1+\beta_4+\beta_7)(\beta_2+\beta_5+\beta_8+\beta_{10}) > (\beta_3+\beta_9)$, the positive equilibrium $E_2(x^*, y^*, s^*)$ is unstable.

Therefore, according to the Hopf bifurcation theory [41], when $m_1 > a_1+1, m_2 > 1, 0 < a_1 < 1$, $v < 0$, $h(n_2^*) \leq 0$, $\beta_1+\beta_4+\beta_7 > 0$, $\beta_3+\beta_9 > 0$ and $(\beta_1+\beta_4+\beta_7)(\beta_2+\beta_5+\beta_8+\beta_{10}) > (\beta_3+\beta_9)$, there exists a $\tau_2^* > 0$. When $\tau_1 = 0$ and $0 \leq \tau_2 < \tau_2^*$, the positive equilibrium $E_2(x^*, y^*, s^*)$ is locally asymptotically stable; when $\tau_1 = 0$ and $\tau_2 = \tau_2^*$, system (1.3) will undergo a Hopf bifurcation; when $\tau_1 = 0$ and $\tau_2 > \tau_2^*$, the positive equilibrium $E_2(x^*, y^*, s^*)$ is unstable. □

3.3.4. The case of $\tau_1 > 0$ and $\tau_2 > 0$

Theorem 3.6. If $\tau_1 > 0, \tau_2 > 0$, $m_1 > a_1+1, m_2 > 1, 0 < a_1 < 1$, $v < 0$, $h(n_2^*) \leq 0, \beta_1+\beta_4+\beta_7 > 0$, $\beta_3+\beta_9 > 0, (\beta_1+\beta_4+\beta_7)(\beta_2+\beta_5+\beta_8+\beta_{10}) > (\beta_3+\beta_9)$ and $0 < \tau_2 < \tau_2^*$, for any $\tau_1 > 0$, the positive equilibrium $E_2(x^*, y^*, s^*)$ is always locally asymptotically stable.

Proof. When $\tau_1 > 0, \tau_2 > 0$, based on Eq.(3.10), we obtain the characteristic equation of system (1.3),

$$f(\lambda) = H_0(\lambda) + H_1(\lambda)e^{-\lambda\tau_1} + H_2(\lambda)e^{-\lambda\tau_2} + H_3(\lambda)e^{-\lambda\tau_1}e^{-\lambda\tau_2} = 0, \tag{3.21}$$

where,

$$H_0(\lambda) = \lambda^3+\beta_1\lambda^2+\beta_2\lambda+\beta_3,\ H_1(\lambda) = \beta_4\lambda^2+\beta_5\lambda+\beta_6,$$
$$H_2(\lambda) = \beta_7\lambda^2+\beta_8\lambda+\beta_9,\ H_3(\lambda) = \beta_{10}\lambda+\beta_{11}.$$

Since $v < 0$, $h(n_2^*) \leq 0, \beta_1+\beta_4+\beta_7 > 0, \beta_3+\beta_9 > 0, (\beta_1+\beta_4+\beta_7)(\beta_2+\beta_5+\beta_8+\beta_{10}) > (\beta_3+\beta_9)$ and $0 \leq \tau_2 < \tau_2^*$, we obtain that τ_2 is the parameter that satisfies the asymptotic stability condition of the positive equilibrium $E_2(x^*, y^*, s^*)$ in Theorem 3.5.(2).

If we regard τ_1 as a branch parameter and let $\lambda = i\omega$ be an eigenvalue of Eq (3.21), we can obtain

$$E_5\cos\omega\tau_1 + F_5\sin\omega\tau_1 - E_6 + i(F_5\cos\omega\tau_1 - E_5\sin\omega\tau_1 - F_6) = 0,$$

where,

$$E_5 = -\beta_4\omega^2+\beta_6+\beta_{10}\omega\sin\omega\tau_2+\beta_{11}\cos\omega\tau_2,\ F_5 = \beta_5+\beta_{10}\omega\cos\omega\tau_2-\beta_{11}\sin\omega\tau_2,$$

$$E_6 = \beta_1\omega^2-\beta_3-(-\beta_7\omega^2+\beta_9)\cos\omega\tau_2-\beta_8\omega\sin\omega\tau_2,$$
$$F_6 = \omega^3-\beta_2\omega+(-\beta_7\omega^2+\beta_9)\sin\omega\tau_2-\beta_8\omega\cos\omega\tau_2.$$

Separating the real and imaginary parts, we get

$$\begin{cases} E_5 \cos \omega\tau_1 + F_5 \sin \omega\tau_1 = E_6, \\ -E_5 \sin \omega\tau_1 + F_5 \cos \omega\tau_1 = F_6. \end{cases}$$

Applying $\sin^2 \omega\tau_1 + \cos^2 \omega\tau_1 = 1$, we obtain a transcendental equation,

$$f(\omega, \tau_2) = {E_5}^2 + {F_5}^2 - {E_6}^2 - {F_6}^2 = 0. \tag{3.22}$$

It is well known that transcendental equations usually do not have exact solutions, and generally the roots of the equations can not be directly determined. Thus, for Eq (3.22), we use numerical calculations and drawing methods to discuss the root situation.

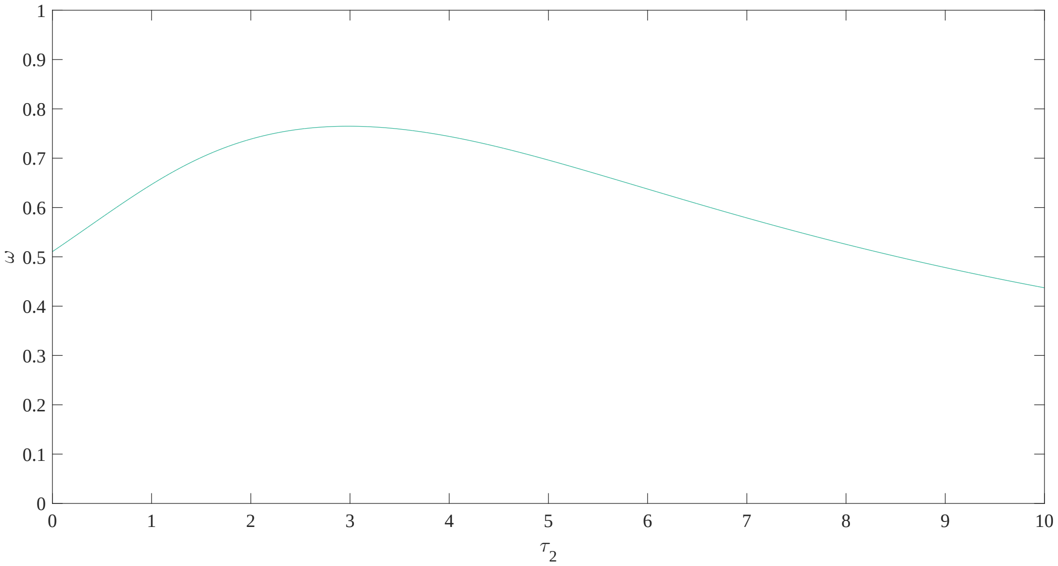

Figure 1. Show the numerical calculation diagram of Eq (3.22) in the interval [0,10] with $m_1 = 8, a_1 = 0.85, m_2 = 3.5, a_2 = 0.95$.

It can be seen from Figure 1 that when $m_1 > a_1 + 1, m_2 > 1, 0 < a_1 < 1$, $v < 0$, $h(n_2^*) \leq 0$, $\beta_1 + \beta_4 + \beta_7 > 0, \beta_3 + \beta_9 > 0, (\beta_1 + \beta_4 + \beta_7)(\beta_2 + \beta_5 + \beta_8 + \beta_{10}) > (\beta_3 + \beta_9)$ and $0 < \tau_2 < \tau_2^*$, the image of Eq (3.22) is always above the horizontal axis. Thus, Eq (3.22) does not have positive roots. At the same time, by the conclusion of Theorem 3.5.(2), we obtain all the roots of Eq (3.21) have negative real parts.

Therefore, when $\tau_1 > 0, \tau_2 > 0$, $m_1 > a_1 + 1, m_2 > 1, 0 < a_1 < 1$, $v < 0$, $h(n_2^*) \leq 0, \beta_1 + \beta_4 + \beta_7 > 0$, $\beta_3 + \beta_9 > 0, (\beta_1 + \beta_4 + \beta_7)(\beta_2 + \beta_5 + \beta_8 + \beta_{10}) > (\beta_3 + \beta_9)$ and $0 \leq \tau_2 < \tau_2^*$, for any $\tau_1 > 0$, the positive equilibrium $E_2(x^*, y^*, s^*)$ is always locally asymptotically stable. □

4. Numerical simulation

In this section, we will give several numerical examples to further verify the correctness of the theoretical analysis in Section 3, which can intuitively show that our proposed control strategy is effective. To this end, we select the delays τ_1 and τ_2 as the bifurcation parameters, fix $s^0 = 1$, $x^0 = 0.5$ and $y^0 = 0.5$ as the initial value conditions and use MATLAB to numerically fit system (1.3). Since the two boundary equilibria are special cases of the positive equilibrium, we will omit it and only discuss the stability and Hopf bifurcation of system (1.3) at the positive equilibrium $E_2(x^*, y^*, s^*)$.

Next, we will provide numerical simulations for each of the four cases in Section 3.3. For the convenience of comparison, the system with delays is represented by a solid line, and the system without delays is represented by a dashed line.

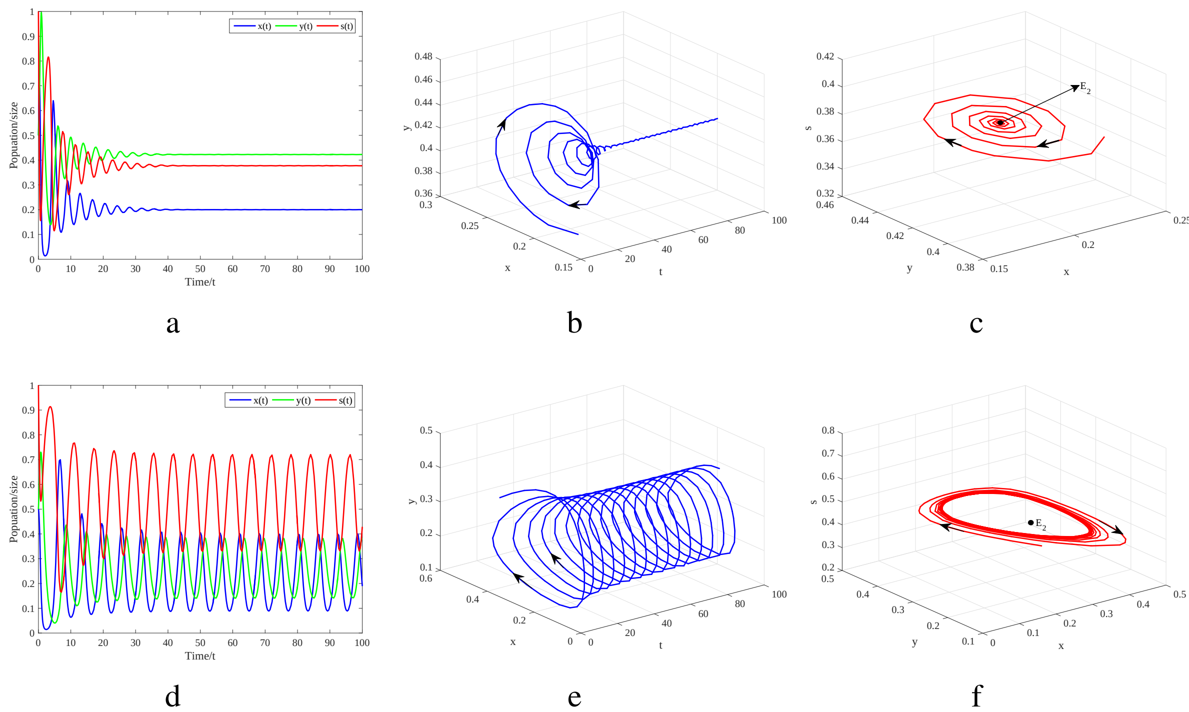

Figure 2. Show the time-series diagram, the time trajectory diagram and the phase diagram of system (1.3) in Case (I) with $\tau_1 = 0$ and $\tau_2 = 0$, where $m_1 = 6, a_1 = 0.35, m_2 = 3.5, a_2 = 0.5$(top) and $m_1 = 3.5, a_1 = 0.35, m_2 = 3.5, a_2 = 0.5$(bottom).

Case (I). When $\tau_1 = 0$ and $\tau_2 = 0$, we fix $m_1 = 6$, $a_1 = 0.35$, $m_2 = 3.5$ and $a_2 = 0.5$, then we calculate $\mathcal{A}_1 \approx 1.1901 > 0$, $\beta_3 + \beta_9 \approx 2.7073 > 0$, $\mathcal{A}_2 \approx 0.7408 > 0$ and $E_2(0.2000, 0.4226, 0.3774)$. It is easy to verify that all system parameters satisfy the conditions of Theorem 3.3. From Figure 2(a) and (b), we see that the time-series graphs of x, y and s and the time trajectory diagram of x and y gradually change from fluctuations to a straight line. In addition, from Figure 2(c), we see that the phase diagrams of x, y and s gradually converge to the positive equilibrium $E_2(0.2000, 0.4226, 0.3774)$. Thus, when the system parameters satisfy the conditions of Theorem 3.3, the positive equilibrium $E_2(0.2000, 0.4226, 0.3774)$ is stable.

On the contrary, if we choose $m_1 = 3.5$, $a_1 = 0.35$, $m_2 = 3.5$ and $a_2 = 0.5$, we calculate that $\mathcal{A}_1 \approx 0.9586 > 0$, $\beta_3 + \beta_9 \approx 1.0739 > 0$, $\mathcal{A}_2 \approx -0.0841 < 0$ and $E_2(0.2000, 0.2329, 0.5671)$. It is easy to verify that the parameters of system (1.3) do not satisfy the conditions of Theorem 3.3. From Figure 2(d), we see that the time-series graphs of x, y and s are in periodic oscillation; from

Figure 2(e), we see that the time trajectories of x and y are spiral; from Figure 2(f), we see that the phase diagrams of x, y and s are in a circle shape and will not converge to the positive equilibrium $E_2(0.2000, 0.2329, 0.5671)$. Thus, when the system parameters do not satisfy the conditions of Theorem 3.3, the positive equilibrium $E_2(0.2000, 0.2329, 0.5671)$ is unstable.

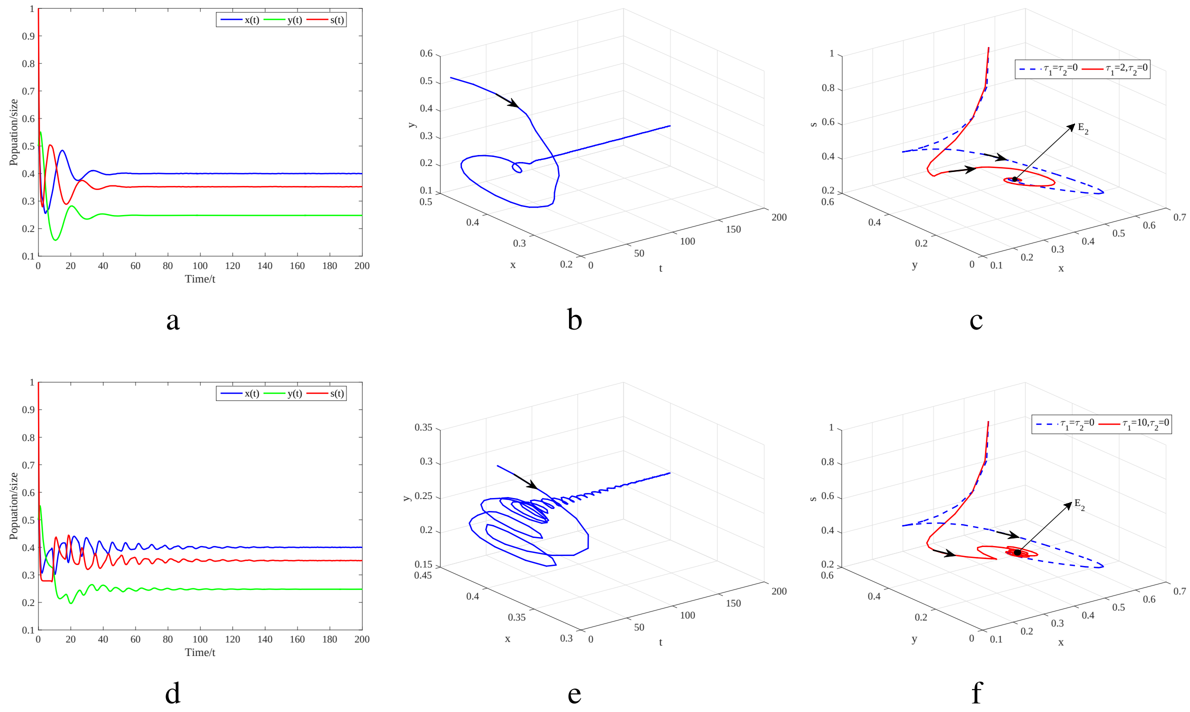

Figure 3. Show the time-series diagram, the time trajectory diagram and the phase diagram of system (1.3) in Case (II) with $m_1 = 3$, $a_1 = 0.3$, $m_2 = 2$ and $a_2 = 0.4$, where $\tau_1 = 2$, $\tau_2 = 0$(top) and $\tau_1 = 10$, $\tau_2 = 0$(bottom).

Case (II). (i) If we fix $m_1 = 3$, $a_1 = 0.3$, $m_2 = 2$ and $a_2 = 0.4$, we calculate that $\mathcal{A}_1 \approx 1.5367 > 0$, $\beta_3 + \beta_9 \approx 0.5723 > 0$, $\mathcal{A}_2 \approx 1.1320 > 0$ and $E_2(0.4000, 0.2479, 0.3521)$. It is easy to verify that the parameters satisfy the conditions of Theorem 3.3. As $q = 1.2099 > 0$ and $p^2 - 3q = -0.0863 < 0$, we know that ω_0 does not have real roots. From Figure 3, we know that no matter choose $\tau_1 = 2 > 0, \tau_2 = 0$ or $\tau_1 = 10 > 0, \tau_2 = 0$, the time-series graphs of x, y and s and the time trajectories of x and y all gradually tend to a straight line, and the phase diagrams of x, y and s in system (1.3) and its corresponding system without delays always converge to the positive equilibrium $E_2(0.4000, 0.2479, 0.3521)$. Thus, when the system parameters satisfy the conditions of Theorem 3.4.(1), for all $\tau_1 > 0, \tau_2 = 0$, the positive equilibrium $E_2(0.4000, 0.2479, 0.3521)$ is stable.

(ii) If we fix $m_1 = 4.5$, $a_1 = 0.45$, $m_2 = 2.5$ and $a_2 = 0.15$, we calculate that $\mathcal{A}_1 \approx 0.4380 > 0$, $\beta_3 + \beta_9 \approx 1.2206 > 0$, $\mathcal{A}_2 \approx -0.9321 < 0$ and $E_2 = (0.1000, 0.1773, 0.7227)$, then it is easy to verify that the parameters do not satisfy the conditions of Theorem 3.3. Moreover, as $q = -3.7527 < 0$ and $h(z_2^*) = -3.2171 < 0$, we know that $\omega_0 \approx 0.5491$ and $\tau_1^* \approx 1.1800$. If we choose $\tau_1 = 0.8 < \tau_1^*$ and $\tau_2 = 0$, from Figure 4(a), we see that the time-series graphs of x, y and s are in periodic oscillation; from Figure 4(b), we see that the time trajectories of x and y are spiral; from Figure 4(c), we see that the phase diagrams of x, y and s in system (1.3) and its corresponding system without delays are in a circle shape and will not converge to the positive equilibrium $E_2 = (0.1000, 0.1773, 0.7227)$. Thus, when $\tau_1 < \tau_1^*$, $\tau_2 = 0$ and the system parameters satisfy the conditions of Theorem 3.4.(2), the positive equilibrium $E_2 = (0.1000, 0.1773, 0.7227)$ is unstable.

On the contrary, if we choose $\tau_1 = 2 > \tau_1^*$ and $\tau_2 = 0$, from Figure 4(d) and (e), we see that the time-series graphs of x, y and s and the time trajectories of x and y tend to a straight line; from Figure 4(f), contrary to the phase diagram of the system without delays, we see that the phase diagrams of x, y and s in system (1.3) gradually converge to the positive equilibrium $E_2(0.1000, 0.1773, 0.7227)$. Thus, when $\tau_1 > \tau_1^*$, $\tau_2 = 0$ and the system parameters satisfy the conditions of Theorem 3.4.(2), the positive equilibrium $E_2(0.1000, 0.1773, 0.7227)$ is stable.

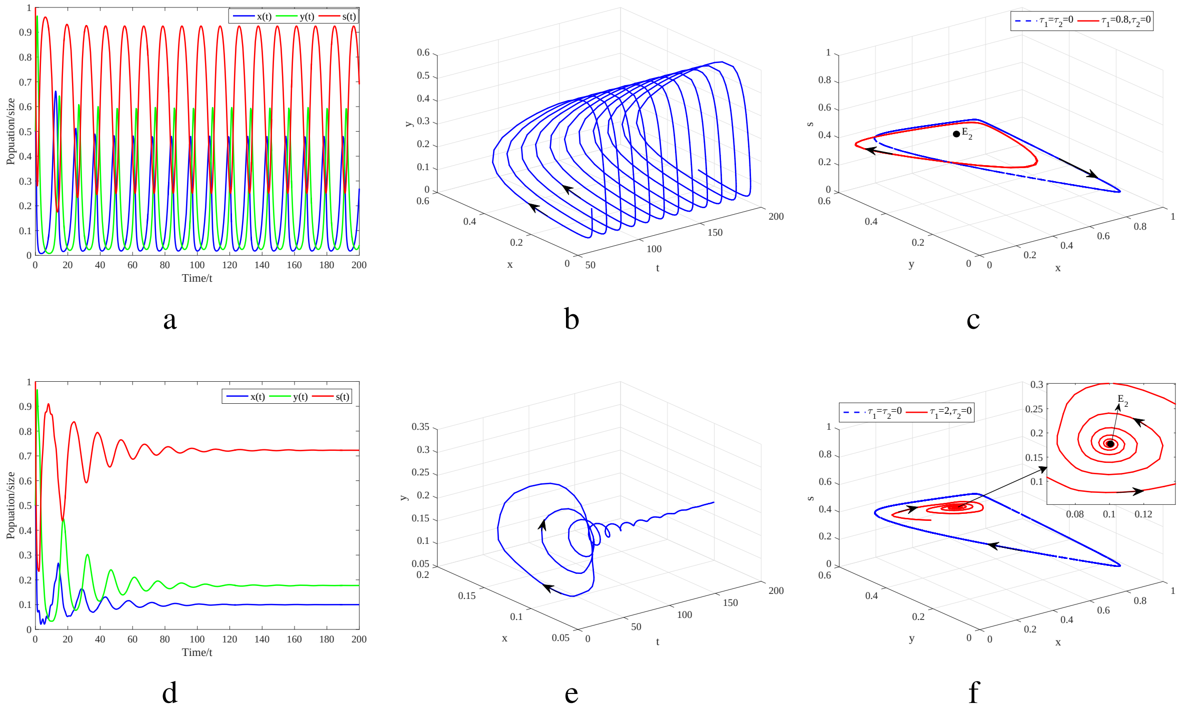

Figure 4. Show the time-series diagram, the time trajectory diagram and the phase diagram of system (1.3) in Case (II) with $m_1 = 4.5$, $a_1 = 0.45$, $m_2 = 2.5$ and $a_2 = 0.15$, where $\tau_1 = 0.8$, $\tau_2 = 0$(top) and $\tau_1 = 2$, $\tau_2 = 0$(bottom).

Case (III). When $\tau_1 = 0$ and $\tau_2 > 0$, we fix $m_1 = 8$, $a_1 = 0.85$, $m_2 = 6$ and $a_2 = 0.95$, then we obtain that $\mathcal{A}_1 \approx 1.4449 > 0$, $\beta_3 + \beta_9 \approx 2.6571 > 0$, $\mathcal{A}_2 \approx 1.8250 > 0$ and $E_2 = (0.1900, 0.3464, 0.4636)$. It satisfies the conditions of Theorem 3.3. Furthermore, as $v = -10.8856 < 0$ and $h(n_2^*) = -7.1856 < 0$, we get $\omega_0 \approx 1.6593$ and $\tau_2^* \approx 0.1173$. If we choose $\tau_1 = 0$ and $\tau_2 = 0.05 < \tau_2^*$, from Figure 5(a) and (b), we see that the time-series graphs of x, y and s and the time trajectories of x and y all tend to a straight line; from Figure 5(c), we see that the phase diagrams of x, y and s in system (1.3) and its corresponding system without delays gradually converge to the positive equilibrium $E_2 = (0.1900, 0.3464, 0.4636)$. Thus, when $\tau_1 = 0$, $0 < \tau_2 < \tau_2^*$ and the system parameters satisfy the conditions of Theorem 3.5.(2), the positive equilibrium $E_2 = (0.1900, 0.3464, 0.4636)$ is stable.

On the contrary, if we choose $\tau_1 = 0$ and $\tau_2 = 0.15 > \tau_2^*$, from Figure 5(d), we see that the time-series graphs of x, y and s are in periodic oscillation; from Figure 5(e), we see that the time trajectories of x and y are spiral; from Figure 5(f), contrary to the phase diagram of the system without delays, we see that the phase diagrams of x, y and s are in a circle shape and will not converge to the positive equilibrium $E_2 = (0.1900, 0.3464, 0.4636)$. Thus, when $\tau_1 = 0$, $\tau_2 > \tau_2^*$ and the system parameters satisfy the conditions of Theorem 3.5.(2), the positive equilibrium $E_2 = (0.1900, 0.3464, 0.4636)$ is unstable.

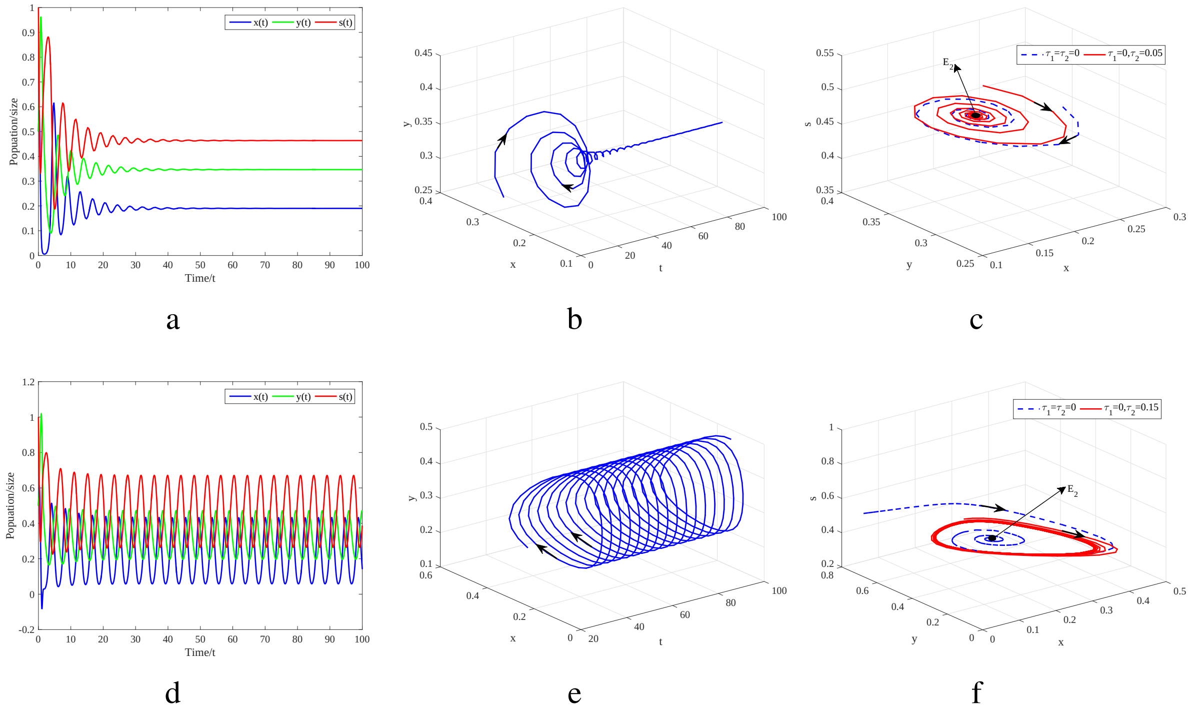

Figure 5. Show the time-series diagram, the time trajectory diagram and the phase diagram of system (1.3) in Case (III) with $m_1 = 8$, $a_1 = 0.85$, $m_2 = 6$ and $a_2 = 0.95$, where $\tau_1 = 0$, $\tau_2 = 0.05 < {\tau_2}^* = 0.1173$(top) and $\tau_1 = 0$, $\tau_2 = 0.15 > {\tau_2}^* = 0.1173$(bottom).

Case (IV). When $\tau_1 > 0$ and $\tau_2 > 0$, we fix $m_1 = 8$, $a_1 = 0.85$, $m_2 = 3.5$ and $a_2 = 0.95$, then we calculate that $\mathcal{A}_1 \approx 2.7995 > 0$, $\beta_3 + \beta_9 \approx 2.0208 > 0$, $\mathcal{A}_2 \approx 8.6742 > 0$ and $E_2(0.3800, 0.3509, 0.2691)$. It is easy to verify that the parameters satisfy the conditions of Theorem 3.6. Moreover, by the numerical results of Theorem 3.5.(ii), we let $\tau_2^* \approx 0.7751$. From Figure 6, we see that whether we choose $\tau_1 = 0.6, \tau_2 = 0.7 < \tau_2^*$ or $\tau_1 = 1, \tau_2 = 0.7 < \tau_2^*$, the time-series graphs of x, y and s and the time trajectories of x and y all tend to a straight line, and the phase diagrams of x, y and s gradually converge to the positive equilibrium. Thus, when the system parameters satisfy the conditions of Theorem 3.6, the positive equilibrium $E_2(0.3800, 0.3509, 0.2691)$ is always stable.

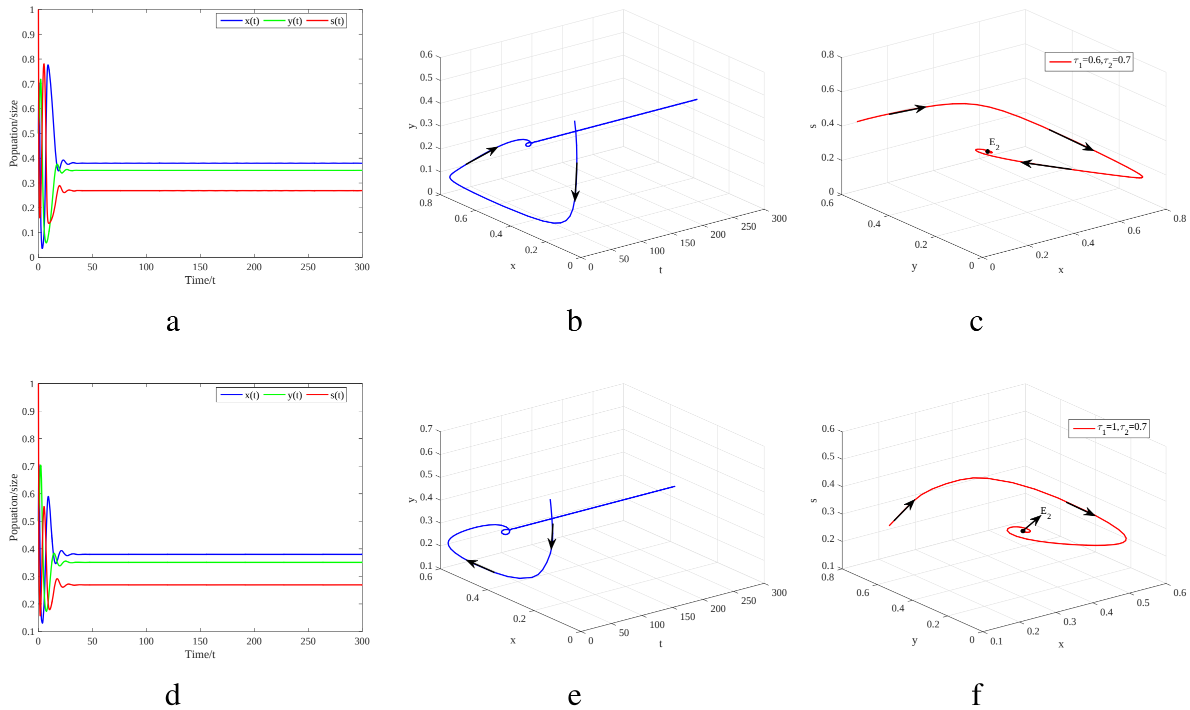

Figure 6. Show the time-series diagram, the time trajectory diagram and the phase diagram of system (1.3) in Case (IV) with $m_1 = 8$, $a_1 = 0.85$, $m_2 = 3.5$ and $a_2 = 0.95$, where $\tau_1 = 0.6, \tau_2 = 0.7$(top) and $\tau_1 = 1, \tau_2 = 0.7$(bottom).

5. Conclusions and discussion

When modeling and analyzing the wastewater biological treatment system, it is more significant to consider time delay models than traditional models without delay. In this paper, we propose a food chain chemostat model with Michaelis-Menten functional response and double delays. Firstly, we analyze the existence conditions of three equilibria in the chemostat model (1.3) and prove the stability conditions of three equilibria $E_0(0, 0, 1)$, $E_1(x_1^*, 0, s_1^*)$ and $E_2(x^*, y^*, s^*)$, respectively. In addition, we obtain the sufficient conditions for system (1.3) to undergo the Hopf bifurcation at the positive equilibrium. In particular, in the numerical simulation, we compare the chemostat model with delays and its corresponding chemostat model without delays.

The results show that time delays will affect the stability of system (1.3) and even lead to Hopf bifurcation. When $m_1 > a_1 + 1$, $m_2 > 1$ and $0 < a_1 < 1$, there are three equilibria $E_0(0, 0, 1)$, $E_1(x_1^*, 0, s_1^*)$ and $E_2(x^*, y^*, s^*)$ in system (1.3), and $E_1(x_1^*, 0, s_1^*)$ is always locally asymptotically stable. As the delays τ_1 and τ_2 change, the stability of the positive equilibrium will undergo stability switches. Especially, when the delays τ_1 and τ_2 are close to the fixed delay $\tau_i^*(i = 1, 2)$, system (1.3) will undergo the Hopf bifurcation; when the delays τ_1 and τ_2 are away from the fixed delay $\tau_i^*(i = 1, 2)$, system (1.3) will become unstable from stable at the positive equilibrium.

It is known that the chemostat has the advantages of measurable experimental parameters, convenient data collection and reasonable experiments. Based on the discussion of Theorem 3.3

to Theorem 3.6, we have obtained sufficient conditions for the stability of the chemostat system at the positive equilibrium, which shows that we can control the cultivation of microorganisms through scientific strategies. If the two different microorganisms in the culture vessel can eventually tend to a stable constant, the culture of the microorganism is successful. If the extinction equilibrium is stable, which means that the cultured microorganisms finally tend to 0, the culture of the microorganism fails. Therefore, in the actual microbial culture, we should try our best to control a_1, a_2, m_1 and m_2 so that they do not satisfy the stability conditions of the extinction equilibrium, which is helpful to cultivate the microorganisms effectively.

There is still much interesting work worthy of our attention on the study of chemostat models in biological wastewater treatment systems, such as the global asymptotic stability of the system, the extinction and persistence of organisms, and the stochastic effects of the environment on microorganisms in wastewater treatment. Especially, fractional-order models with time delay are novel and valuable. It can be applied to describe the memory and genetic properties inherent in various processes that exist in most biological systems and can enable established ecological models with greater spatial and temporal freedom. Thus, inspired by the reference [45], we will extend model (1.3) to the following chemostat model with fractional-order delay,

$$\begin{cases} \mathcal{D}^{\alpha}x(t) = \frac{m_1 s(t)x(t-\tau_1)}{a_1+s(t)} - x(t) - \frac{m_2 y(t-\tau_2)x(t-\tau_2)}{a_2+x(t-\tau_2)}, \\ \mathcal{D}^{\alpha}y(t) = \frac{m_2 x(t-\tau_2)y(t-\tau_2)}{a_2+x(t-\tau_2)} - y(t), \\ \mathcal{D}^{\alpha}s(t) = 1 - s(t) - \frac{m_1 s(t)x(t-\tau_1)}{a_1+s(t)}. \end{cases} \tag{5.1}$$

If $\alpha = 1$, model (5.1) can further derive the results of model (1.3) studied in this paper. The related discussions are in progress.

Acknowledgments

This research was funded by the National College Students' Innovation and Entrepreneurship Training Program (S202110619028); School of Science College Student Innovation Fund Project of Southwest University of Science and Technology (LX2020005); Application Basic Project of Sichuan Science and Technology Department (2017JY0336); Longshan Academic Talent Research Support Program of Southwest University of Science and Technology (17LZX670, 18LZX622).

Conflict of interest

The authors declare there is no conflict of interests.

References

1. H. L. Smith, P. Waltman, *The theory of the chemostat: dynamics of microbial competition*, Cambridge University Press, 1995.
2. V. Sree Hari Rao, P. Raja Sekhara Rao, Basic chemostat model revisited, *Differ. Equ. Dyn. Syst.*, **17** (2009), 3–16. http://dx.doi.org/10.1007/s12591-009-0001-2
3. H. Veldkamp, Ecological studies with the chemostat, In: *Advances in microbial ecology*, Boston, MA: Springer, 1977: 59–94. http://dx.doi.org/10.1007/978-1-4615-8219-9_2

4. P. Praveen, D. T. T. Nguyen, K. C. Loh, Biodegradation of phenol from saline wastewater using forward osmotic hollow fiber membrane bioreactor coupled chemostat, *Biochem. Eng. J.*, **94** (2015), 125–133. https://doi.org/10.1016/j.bej.2014.11.014

5. D. H. Nguyen, N. N. Nguyen, G. Yin, General nonlinear stochastic systems motivated by chemostat models: Complete characterization of long-time behavior, optimal controls, and applications to wastewater treatment, *Stoch. Proc. Appl.*, **130** (2020), 4608–4642. https://doi.org/10.1016/j.spa.2020.01.010

6. M. Ahmed, A. Mydlarczyk, A. Abusam, Kinetic modeling of GAC-IFAS chemostat for petrochemical wastewater treatment, *Journal of Water Resource and Hydraulic Engineering*, **6** (2017), 27–33. https://doi.org/10.5963/JWRHE0602002

7. A. Novick, L. Szilard, Description of the chemostat, *Science*, **112** (1950), 715–716. https://doi.org/10.1126/science.112.2920.715

8. Z. P. Qiu, J. Yu, Y. Zou, The asymptotic behavior of a chemostat model with the Beddington-DeAngelis functional response, *Math. Biosci.*, **187** (2004), 175–187. https://doi.org/10.1016/j.mbs.2003.10.001

9. L. Imhof, S. Walcher, Exclusion and persistence in deterministic and stochastic chemostat models, *J. Differ. Equations*, **217** (2005), 26–53. https://doi.org/10.1016/j.jde.2005.06.017

10. H. Nie, J. H. Wu, Coexistence of an unstirred chemostat model with Beddington-DeAngelis functional response and inhibitor, *Nonlinear Anal. Real*, **11** (2010), 3639–3652. https://doi.org/10.1016/j.nonrwa.2010.01.010

11. L. Zou, X. W. Chen, S. G. Ruan, W. N. Zhang, Dynamics of a model of allelopathy and bacteriocin with a single mutation, *Nonlinear Anal. Real*, **12** (2011), 658–670. https://doi.org/10.1016/j.nonrwa.2010.07.008

12. C. Q. Xu, S. L. Yuan, An analogue of break-even concentration in a simple stochastic chemostat model, *Appl. Math. Lett.*, **48** (2015), 62–68. https://doi.org/10.1016/j.aml.2015.03.012

13. D. Herbert, R. Elsworth, R. C. Telling, The continuous culture of bacteria; a theoretical and experimental study, *Journal of General Microbiology*, **14** (1956), 601–622. https://doi.org/10.1099/00221287-14-3-601

14. L. Michaelis, M. L. Menten, Die kinetik der invertinwirkung, *Biochemische Zeitschrift*, **49** (1913), 333–369.

15. C. P. L. Grady Jr, G. T. Daigger, N. G. Love, C. D. M. Filipe, *Biological wastewater treatment*, CRC press, 2011.

16. B. Li, Y. Kuang, Simple food chain in a chemostat with distinct removal rates, *J. Math. Anal. Appl.*, **242** (2000), 75–92. https://doi.org/10.1006/jmaa.1999.6655

17. L. Wang, D. Jiang, Ergodicity and threshold behaviors of a predator-prey model in stochastic chemostat driven by regime switching, *Math. Method. Appl. Sci.*, **44** (2021), 325–344. https://doi.org/10.1002/mma.6738

18. E. Ali, M. Asif, A. H. Ajbar, Study of chaotic behavior in predator–prey interactions in a chemostat, *Ecol. Model.*, **259** (2013), 10–15. https://doi.org/10.1016/j.ecolmodel.2013.02.029

19. G. Rajchakit, R. Sriraman, C. P. Lim, B. Unyong, Existence, uniqueness and global stability of clifford-valued neutral-type neural networks with time delays, *Math. Comput. Simulat.*, in press. https://doi.org/10.1016/j.matcom.2021.02.023
20. R. Xu, Global dynamics of an SEIRI epidemiological model with time delay, *Appl. Math. Comput.*, **232** (2014), 436–444. https://doi.org/10.1016/j.amc.2014.01.100
21. C. Huang, H. Zhang, J. Cao, H. Hu, Stability and Hopf bifurcation of a delayed prey-predator model with disease in the predator, *Int. J. Bifurcat. Chaos*, **29** (2019), 1950091. https://doi.org/10.1142/S0218127419500913
22. X. W. Jiang, X. Y. Chen, M. Chi, J. Chen, On Hopf bifurcation and control for a delay systems, *Appl. Math. Comput.*, **370** (2020), 124906. https://doi.org/10.1016/j.amc.2019.124906
23. W. Qi, G. Zong, H. R. Karimi, L_∞ control for positive delay systems with semi-Markov process and application to a communication network model, *IEEE Trans. Ind. Electron.*, **66** (2018), 2081–2091. https://doi.org/10.1109/TIE.2018.2838113
24. H. Y. Zhao, N. Ding, Dynamic analysis of stochastic Cohen-Grossberg neural networks with time delays, *Appl. Math. Comput.*, **183** (2006), 464–470. https://doi.org/10.1016/j.amc.2006.05.087
25. Q. K. Song, Z. D. Wang, An analysis on existence and global exponential stability of periodic solutions for BAM neural networks with time-varying delays, *Nonlinear Anal. Real*, **8** (2007), 1224–1234. https://doi.org/10.1016/j.nonrwa.2006.07.002
26. C. Huang, J. Cao, M. Xiao, A. Alsaedi, T. Hayat, Bifurcations in a delayed fractional complex-valued neural network, *Appl. Math. Comput.*, **292** (2016), 210–227. https://doi.org/10.1016/j.amc.2016.07.029
27. Y. Xiao, L. Chen, An SIS epidemic model with stage structure and a delay, *Acta Mathematicae Applicatae Sinica, English Series*, **18** (2002), 607–618. https://doi.org/10.1007/s102550200063
28. T. Zhang, J. Liu, Z. Teng, Stability of Hopf bifurcation of a delayed SIRS epidemic model with stage structure, *Nonlinear Anal. Real*, **11** (2010), 293–306. https://doi.org/10.1016/j.nonrwa.2008.10.059
29. L. Zhu, G. Guan, Y. Li, Nonlinear dynamical analysis and control strategies of a network-based SIS epidemic model with time delay, *Appl. Math. Model.*, **70** (2019), 512–531. https://doi.org/10.1016/j.apm.2019.01.037
30. Y. Song, J. Wei, Local Hopf bifurcation and global periodic solutions in a delayed predator-prey system, *J. Math. Anal. Appl.*, **301** (2005), 1–21. https://doi.org/10.1016/j.jmaa.2004.06.056
31. F. Li, H. Li, Hopf bifurcation of a predator-prey model with time delay and stage structure for the prey, *Math. Comput. Model.*, **55** (2012), 672–679. https://doi.org/10.1016/j.mcm.2011.08.041
32. X. Jiang, X. Chen, T. Huang, H. Yan, Bifurcation and control for a predator-prey system with two delays, *IEEE Trans. Circuits Syst. II*, **68** (2020), 376–380. https://doi.org/10.1109/TCSII.2020.2987392
33. S. Ruan, G. S. K. Wolkowicz, Bifurcation analysis of a chemostat model with a distributed delay, *J. Math. Anal. Appl.*, **204** (1996), 786–812. https://doi.org/10.1006/jmaa.1996.0468
34. G. S. K. Wolkowicz, H. Xia, Global asymptotic behavior of a chemostat model with discrete delays, *SIAM J. Appl. Math.*, **57** (1997), 1019–1043. https://doi.org/10.1137/S0036139995287314

35. B. Tian, S. Zhong, N. Chen, X. Liu, Impulsive control strategy for a chemostat model with nutrient recycling and distributed time-delay, *Math. Method. Appl. Sci.*, **37** (2018), 496–507. https://doi.org/10.1002/mma.2807

36. S. Sun, C. Guo, X. Liu, Hopf bifurcation of a delayed chemostat model with general monotone response functions, *Comp. Appl. Math.*, **37** (2018), 2714–2737. https://doi.org/10.1007/s40314-017-0476-3

37. X. Yu, S. Yuan, Asymptotic properties of a stochastic chemostat model with two distributed delays and nonlinear perturbation, *Discrete Cont. Dyn. Syst. B*, **25** (2020), 2373–2390. https://doi.org/10.3934/dcdsb.2020014

38. J. K. Hale, S. M. Verduyn Lunel, *Introduction of functional differential equations*, New York: Springer, 1993. https://doi.org/10.1007/978-1-4612-4342-7

39. S. B. Hsu, *Ordinary differential equations with applications*, 2 Eds., World Scientific Publishing Company, 2013. https://doi.org/10.1142/8744

40. S. Ruan, J. Wei, On the zeros of transcendental functions with applications to stability of delay differential equations with two delays, *Dynamics of Continuous, Discrete and Impulsive Systems Series A: Mathematical Analysis*, **10** (2003), 863–874.

41. B. D. Hassard, N. D. Kazarinoff, Y. H. Wan, *Theory and applications of Hopf bifurcation*, Cambridge: Cambridge University Press, 1981.

42. H. I. Freedman, Y. Kuang, Stability switches in linear scalar neutral delay equations, *Funkc. Ekvacioj*, **34** (1991), 187–209.

43. O. Tagashira, T. Hara, Delayed feedback control for a chemostat model, *Math. Biosci.*, **201** (2006), 101–112. https://doi.org/10.1016/j.mbs.2005.12.014

44. Y. Kuang, *Delay differential equations with applications in population dynamics*, Boston: Academic Press, 1993.

45. F. A. Rihan, C. Rajivganthi, Dynamics of fractional-order delay differential model of prey-predator system with Holling-type III and infection among predators, *Chaos Soliton. Fract.*, **141** (2020), 110365. https://doi.org/10.1016/j.chaos.2020.110365

AIMS Press